AFOSR-TR-97-0683

REPORT DOCUMENTATION PAGE

Form Approved OMB No. 0704-0188

1. AGENCY USE ONLY *(Leave blank)*	2. REPORT DATE	3. REPORT TYPE AND DATES COVERED
	27 October 1997	Final Technical Report 1 Apr 95 to 31 Mar 97

4. TITLE AND SUBTITLE
Nonlinear Aeroelastic Effects in Damaged Composite Aerospace Structures

5. FUNDING NUMBERS
F49620-95-1-0241

6. AUTHOR(S)
O. A. Bauchau
R. G. Loewy

7. PERFORMING ORGANIZATION NAME(S) AND ADDRESS(ES)
Georgia Institute of Technology
School of Aerospace Engineering
Atlanta, GA 30332-0150

8. PERFORMING ORGANIZATION REPORT NUMBER

9. SPONSORING/MONITORING AGENCY NAME(S) AND ADDRESS(ES)
AFOSR/NA
110 Duncan Avenue, Rm B115
Bolling AFB, DC 20332-8050

10. SPONSORING/MONITORING AGENCY REPORT NUMBER
F49620-95-1-0241

11. SUPPLEMENTARY NOTES

12a. DISTRIBUTION AVAILABILITY STATEMENT
Approved for Public Release; distribution Unlimited.

12b. DISTRIBUTION CODE

13. ABSTRACT *(Maximum 200 words)*

Matrix micro-cracking affects the stiffness properties of composite laminates and the corresponding sectional stiffnesses, most prominantly laminates exhibiting elastic coupling. Matrix micro-cracking gives rise to nonlinear materials behavior in the presence of nonuniformly distributed crack densities. Such matrix damage appears to have little effect on basic bending-torsion flutter speed. However, this damage can induce a limit cycle behavior at airspeeds somewhat below the flutter speed. The effect of damage on the aeroelastic behavior of wing-aileron systems is found to be more pronounced. Here again flutter speeds were found to be slightly lower in the presence of damage. However, in this case, a limit cycle bahavior was observed for a significant range of airspeeds below the flutter speed. Reduced fatigue life could result from this limit cycle behavior, since much higher cyclic stresses are generated thereby in the wing-aileron structure.

14. SUBJECT TERMS			15. NUMBER OF PAGES
			16. PRICE CODE
17. SECURITY CLASSIFICATION OF REPORT	18. SECURITY CLASSIFICATION OF THIS PAGE	19. SECURITY CLASSIFICATION OF ABSTRACT	20. LIMITATION OF ABSTRACT
Unclassified	Unclassified	Unclassified	UL

Nonlinear Aeroelastic Effects in Damaged Composite Aerospace Structures.

AFOSR Grant #F49620-95-1-0241, Major Brian Sanders, contract monitor.

O. A. Bauchau and R.G. Loewy.

Georgia Institute of Technology.

School of Aerospace Engineering,

Atlanta, Georgia, 30332-0150.

October 27, 1997

Research Objectives

Although aerospace vehicle structures are being designed making greater use of advanced filamentary composite materials than ever before, virtually all the composites in current use are designed to carry the major loads in the fibers. That is, matrix material is left largely unloaded. Nevertheless, the integrity of the matrix material plays important structural roles beyond the fundamental ones of transferring tensile loads around imperfections or damage in an individual fiber reinforcement and shear stresses from one ply to another. Matrix constraint of fiber deflection in transverse directions is a key factor in preventing buckling

of plies under compressive loads. Such local instabilities are, of course, a principal adverse consequence of delamination.

Composites designed and used so as to have no major loads in the matrix material can not provide elastic couplings, and there is a widespread agreement that elastic couplings (e.g. bending/torsion or extension/torsion) can have substantial benefits [1]. Examples include stabilizing the static aeroelastic divergence of forward swept wings and eliminating dynamic instabilities encountered by advanced helicopter rotor blades. Elastic couplings, in general, require loading the matrix material in composite laminates.

The first part of this research investigated the nonlinear aeroelastic behavior of wing structures in the presence of likely and certain unavoidable damage in matrix materials. The investigation focused on matrix micro-cracking which inevitably exists in both resin matrix and metal matrix composites. While micro-cracking of the matrix has a modest effect on the overall elastic properties of composite structures now in service because these composites are designed so that matrix materials are substantially unloaded, their effect on the aeroelastic behavior of structures tailored to provide elastic couplings can be substantial. Micro-cracking was shown [2] to give rise to limit cycle oscillations in nonlinear bi-modular flutter of damaged composite panel.

From an operational standpoint, routine inspection will only detect the most serious damage types, and maintenance programs involving complete structural inspections only take place after many flight hours. As a result, deterioration of aeroelastic properties can go undetected for extended periods of time, and aircrafts flying in such conditions could have significantly reduced stability boundaries.

Both micro-cracking and delamination are damage processes that can lead to nonlinear material behavior and possible nonlinear aeroelastic phenomena. A fundamental difference exists between these two damage mechanisms. Micro-cracking is an unavoidable phenomenon associated with curing stresses and the repeated application of service loads. After a some time in service, a "shake-down" state is reached where significant micro-cracking is present throughout the structure. On the other hand, delamination is a localized phenomenon re-

sulting from foreign object damage, manufacturing defects, or the coalescence of extensive micro-cracking. Delaminations can appear between the layers of a laminate, and under specific loading conditions, these delaminations can grow. Though the size of the delamination can become large when compared to ply or laminate thickness, it is unlikely that this damage will become large when compared to the size of the overall structure without being detected by routine structural inspection. As a result, studying the aeroelastic behavior of wings with delaminations extending over half the span, for instance, would be an academic exercise. On the other hand, the aeroelastic behavior of wings with significant, but localized delaminations is unlikely to be different from that of undamaged wings because a localized delamination only results in a very small change in overall wing stiffness.

There are cases, however, where delaminations can occur over large portions of structural components such as control surfaces, for instance. A given size delamination initiated by foreign object impact could be fairly small compared to wing size, but rather large with respect to aileron or rudder size. Furthermore, the rather high stiffness of actuators, placed so as to be close to the surface being driven, makes for relatively high frequency control surface rotation characteristics. Finally, control surfaces being lighter gage structures are often designed by stiffness rather strength criteria, and the damage caused by an impact of given energy level is likely to result in a more dramatic stiffness reduction for such components. As a result, the second part of this research was devoted to the study of the aeroelastic behavior of wing-aileron structures in the presence of delamination damage.

Reseach Findings

Matrix micro-cracking of composite laminates was found to have a modest effect on the sectional stiffnesses of wings, and on the resulting aeroelastic behavior, though the effect can be very significant on elastic coupling terms. A complicating effect of matrix micro-cracking is that it gives rise to nonlinear material constitutive laws in the presence of nonuniformly distributed crack densities. In particular, nonlinear, bi-modular sectional stiffness properties

are likely to occur in practical situations.

Matrix damage does not seem to have a significant influence on the flutter speed. But for the aeroelastic response to a sharp edged gust, a clear qualitative difference exists between the aeroelastic reponses of the undamaged and damaged wings. The undamaged wing exhibits strong aerodynamic damping characteristics, whereas large amplitude, undamped aeroelastic oscillations, typical of a limit cycle behavior, were observed for the damaged case. At speeds close to, but lower than the flutter speed the peak-to-peak amplitudes for the associated oscillatory root shear force and bending moment are predicted to be as much as an order of magnitude larger for the damaged wing as compared to the undamaged wing. This limit cycle behavior seems to disappear at lower air speeds.

Using a three-dimensional aerodynamic and structural model to simulate wing-aileron flutter when localized delaminations are present, it has been found that the flutter speed of the damaged structure is approximately the same as that of the undamaged structure. But, for a significant range of speed below flutter, high-amplitude oscillations are observed, typical of a limit cycle behavior. These oscillations induce high-amplitude, cyclic stresses in the aileron and at the wing root, that could significantly reduce the fatigue life of the entire structure.

References

[1] Ehlers, S.M. and Weisshaar, T.A., "Adaptive Wing Flexural Axis Control." *Proceedings of the Third International Conference on Adaptive Structures*, San Diego, CA, Nov 9-11, 1992, pp 28-40.

[2] Kim T. Atluri S.N., and Loewy R.G., "Modeling of Micro-Crack Damaged Composite Plates Undergoing Nonlinear Bi-Modular Flutter." *AIAA Journal*, To appear.

Nonlinear Aeroelastic Effects in Damaged Composite Aerospace Structures.

O. A. Bauchau*, B. Douxchamps†, H.C. Zhang‡, and R.G. Loewy§

Georgia Institute of Technology.

School of Aerospace Engineering,

Atlanta, Georgia, 30332-0150.

Abstract

Matrix micro-cracking affects the stiffness properties of composite laminates and the corresponding sectional stiffnesses, most prominantly laminates exhibiting elastic coupling. Matrix micro-cracking gives rise to nonlinear material behavior in the presence of nonuniformly distributed crack densities. Such matrix damage appears to have little effect on basic bending-torsion flutter speed. However, this damage can induce a limit cycle behavior at airspeeds somewhat below the flutter speed. The effect of damage on the aeroelastic behavior of wing-aileron systems is found to be more pronounced. Here again flutter speeds were found to be slightly lower in the presence of damage. However, in this case, a limit cycle behavior was observed for a significant range of airspeeds below the flutter speed. Reduced

[1]Professor

[2]Graduate Research Assistant

[3]Graduate Research Assistant

[4]Professor and Chair

fatigue life could result from this limit cycle behavior, since much higher cyclic stresses are generated thereby in the wing-aileron structure.

1 Introduction

Although aerospace vehicle structures are being designed making greater use of advanced filamentary composite materials than ever before, virtually all the composites in current use are designed to carry the major loads in the fibers. That is, matrix material is left largely unloaded. Nevertheless, the integrity of the matrix material plays important structural roles beyond the fundamental ones of transferring tensile loads around imperfections or damage in an individual fiber reinforcement and shear stresses from one ply to another. Matrix constraint of fiber deflection in transverse directions is a key factor in preventing buckling of plies under compressive loads. Such local instabilities are, of course, a principal adverse consequence of delamination.

Composites designed and used so as to have no major loads in the matrix material can not provide elastic couplings, and there is a widespread agreement that elastic couplings (e.g. bending/torsion or extension/torsion) can have substantial benefits [1]. Examples include stabilizing the static aeroelastic divergence of forward swept wings and eliminating dynamic instabilities encountered by advanced helicopter rotor blades. Elastic couplings, in general, require loading the matrix material in composite laminates.

The first part of this paper will investigate the nonlinear aeroelastic behavior of wing structures in the presence of likely and certain unavoidable damage in matrix materials. The investigation will focus on matrix micro-cracking which inevitably exists in both resin matrix and metal matrix composites. While micro-cracking of the matrix has a modest effect on the overall elastic properties of composite structures now in service because these composites are designed so that matrix materials are substantially unloaded, their effect on the aeroelastic behavior of structures tailored to provide elastic couplings can be substantial. Micro-cracking was shown [2] to give rise to limit cycle oscillations in nonlinear bi-modular

flutter of damaged composite panel.

From an operational standpoint, routine inspection will only detect the most serious damage types, and maintenance programs involving complete structural inspections only take place after many flight hours. As a result, deterioration of aeroelastic properties can go undetected for extended periods of time, and aircrafts flying in such conditions could have significantly reduced stability boundaries.

Both micro-cracking and delamination are damage processes that can lead to nonlinear material behavior and possible nonlinear aeroelastic phenomena. A fundamental difference exists between these two damage mechanisms. Micro-cracking is an unavoidable phenomenon associated with curing stresses and the repeated application of service loads. After a some time in service, a "shake-down" state is reached where significant micro-cracking is present throughout the structure. On the other hand, delamination is a localized phenomenon resulting from foreign object damage, manufacturing defects, or the coalescence of extensive micro-cracking. Delaminations can appear between the layers of a laminate, and under specific loading conditions, these delaminations can grow. Though the size of the delamination can become large when compared to ply or laminate thickness, it is unlikely that this damage will become large when compared to the size of the overall structure without being detected by routine structural inspection. As a result, studying the aeroelastic behavior of wings with delaminations extending over half the span, for instance, would be an academic exercise. On the other hand, the aeroelastic behavior of wings with significant, but localized delaminations is unlikely to be different from that of undamaged wings because a localized delamination only results in a very small change in overall wing stiffness.

There are cases, however, where delaminations can occur over large portions of structural components such as control surfaces, for instance. A given size delamination initiated by foreign object impact could be fairly small compared to wing size, but rather large with respect to aileron or rudder size. Furthermore, the rather high stiffness of actuators, placed so as to be close to the surface being driven, makes for relatively high frequency control surface rotation characteristics. Finally, control surfaces being lighter gage structures are often

designed by stiffness rather strength criteria, and the damage caused by an impact of given energy level is likely to result in a more dramatic stiffness reduction for such components. As a result, the second part of this paper is devoted to the study of the aeroelastic behavior of wing-aileron structures in the presence of delamination damage.

2 Aeroelastic behavior of micro-cracked wing structures

The aeroelastic behavior of wing structures with micro-cracked laminates will be discussed first. The reduced stiffness of the micro-cracked laminate is evaluated using the self-consistent model developed by Dvorak *et al.* [3]. Micro-cracking distribution have been shown to cause nonlinear load-deflection characteristics in bending of laminates and wings [4], although this damage does not affect the load carrying capability of the laminates since there is no fiber breakage.

2.1 Damage Model

When the reinforcing fiber diameter in a composite can be assumed to be much smaller than the micro-crack length, the self-consistent, two-phase model developed by Dvorak *et al.* [3] can be used to evaluate the effect of micro-cracks on the stiffness characteristics of unidirectional plies. The micro-crack density is measured by the parameter $\beta = t/s$, where t is the ply thickness and s is the distance between two adjacent cracks in the ply. The crack distribution in the ply is assumed to be uniform. $\beta = 0$ corresponds to the undamaged state of the ply where no cracks are present. As β increases, an increasing number of cracks appears in the ply, corresponding to an increasing amount of damage. When $\beta = 1$ a saturation level is reached where the distance between cracks is equal to the thickness of the ply; all transverse stresses are relieved by the cracks and there is no driving force to create further cracking. Hence, the range of β is from 0, *i.e.* undamaged matrix, to 1, *i.e.* matrix with a saturated micro-crack level.

The cracked unidirectional composite can be regarded as an orthotropic homogeneous solid on the macroscopic scale. The constitutive equations of the cracked composite are:

$$\underline{\sigma} = L\,\underline{\epsilon}, \quad \underline{\epsilon} = M\,\underline{\sigma}; \tag{1}$$

where L and M are the overall stiffness and compliance matrices of the cracked unidirectional ply, respectively; and $\underline{\sigma}$ and $\underline{\epsilon}$ the average stress and strain in the composite ply, respectively. These compliance matrices are given by:

$$L = L_0 - \frac{1}{4}\pi\beta L_0 \Lambda L, \quad M = M_0 + \frac{1}{4}\pi\beta\Lambda; \tag{2}$$

where L_0 and M_0 are the stiffness and compliance matrices for the uncracked ply, respectively, and the matrix Λ has only three nonzero components

$$\Lambda_{22} = \frac{M_{11}M_{22} - M_{12}^2}{M_{11}}(\alpha_1^{1/2} + \alpha_2^{1/2}); \quad \Lambda_{66} = \sqrt{M_{55}M_{66}}; \tag{3}$$

$$\Lambda_{44} = \frac{\sqrt{M_{11}M_{22} - M_{12}^2}\sqrt{M_{11}M_{33} - M_{13}^2}}{M_{11}}(\alpha_1^{1/2} + \alpha_2^{1/2}); \tag{4}$$

where α_1 and α_2 are the roots of the following equation:

$$(M_{11}M_{22} - M_{12}^2)\alpha^2 - [M_{11}M_{44} + 2(M_{11}M_{13} - M_{12}M_{13})]\alpha + M_{11}M_{33} - M_{13}^2 = 0. \tag{5}$$

A simple iterative procedure involving eqs. (2) though (5) is used to determine the stiffness and compliance matrices of a damaged ply given a micro-crack density β.

2.2 Wing Configuration

The unique directional properties of composites can be exploited in several different ways to achieve specific goals. For instance, aeroelastic tailoring of wings can be used to achieve twist and/or camber control, and flutter or divergence control. This work will focus on an elastically tailored, small scale wing investigated within the framework of NASA's Highly Maneuverable Technology program. A description of material properties, laminate configuration, and beam geometries used in this program are found in [5]. Composite beams using

Hercules AS3501-5A graphite/epoxy material were constructed with the following laminate sequence: [44.5% 15°, 44.5% 55°, 11% 20°]. A 0° fiber orientation is aligned with the axis of the beam. A box beam was constructed with upper and lower faces made of the above laminates, held together by aluminum C-channels and honeycomb core. The cross-section has a width of 280 mm and a depth of 32 mm. The beam length is 2.5 m. The beam has bending-twisting coupling resulting from the unbalanced angle plies. As discussed in [5], such elastic coupling can be used to control the aeroelastic divergence of a forward swept wing. If matrix cracking has an effect on the aeroelastic behavior of composite structures, the largest effect is likely to be found when dealing with such elastically tailored structures.

The damage model described in the previous section is used to evaluate the changes in compliance of the unidirectional plies as a function of the micro-cracking density. Fig. 1 shows the drop in unidirectional ply stiffness properties as a function of crack density. The sectional properties of the beam were then computed using the finite element model developed by Borri *et al.* [6].

Table 1 lists the torsional and bending compliances of the beam without and with micro-cracked matrices. For the micro-cracked beam, two cases were considered: in the first case (Case 1) both upper and lower faces are saturated by micro-cracks (*i.e.* $\beta = 1$ in both upper and lower faces), in the second case (Case 2) only the lower face is damaged (*i.e.* $\beta = 0$ in the upper face and $\beta = 1$ in the lower face). The first case describes the worst possible situation, though such a damage is unlikely to occur in practical operations. The second case is more realistic: only the lower face develops micro-cracks as a result of the repeated application of tensile flight loads and the upper face, subjected primarily to compressive flight loads, remains relatively free of micro-cracks. Sectional stiffnesses show a pronounced dependency on damage: a nearly 40% drop in coupling compliance is predicted in even this more practical case.

2.3 Aeroelastic Analysis Results

Aeroelastic analyses were first performed based on a simple model of the wing. The structural model is based on a finite element multi-body dynamics formulation [10]. Four cubic beam elements were used to model the wing. The aerodynamic forces were computed using a simple, two-dimensional quasi-steady approximation, since the effect of nonlinear structural behavior on flutter characteristics was the matter of interest, rather than accurate prediction of the flutter speed itself. These forces are computed at 12 equally spaced locations along the wing.

At first, the flutter speed of the undamaged and damaged wing were computed. The flutter speed was found to be 122.5 m/sec in the absence of damage. For the damaged wing, Case 1 sectional properties were used; the flutter speed decreased by 6.0%. This fairly small decrease in flutter speed reflects the modest decrease in sectional stiffness properties. This result, in fact, could have been readily predicted based on the formula for simple, two-degree-of-freedom flutter models [7].

Next, the aeroelastic response of this wing to a sharp edged gust is presented. The initial conditions are taken as the aeroelastic equilibrium position of the wing at a 1° angle of attack, with a far field flow velocity at 90% of the flutter speed, *i.e.* 110 m/sec. At the beginning of the simulation, the wing encounters an updraft $W = 8.5\ m/sec$ and the subsequent aeroelastic response is computed.

The sectional stiffnesses are determined according to the following criterion: if bending curvature is down, the cracks in the lower face close and constant, undamaged properties are used; if the bending curvature is up, the cracks in the lower face will open, and constant, damaged properties Case 2 are used. This results in nonlinear, bi-modular sectional stiffness properties as depicted in Fig. 2. To avoid a sudden jump in properties at zero curvatures, a smooth transition, consisting of a simple cubic polynomial, was used between the two stiffness values. The extent of this transition zone is determined by the non-dimensional parameter σ which is the ratio of the transition zone size to that of the entire range of curvatures values during the simulation; $\sigma = 0.01$ will be used in the present simulations.

Figs. 3, 4, and 5 show the time history of the wing gust response tip rotations, root shear force, and root bending moment, respectively. These figures show that a sharp qualitative difference exists between the aeroelastic reponses of the undamaged and damaged wings. The undamaged wing presents strong aerodynamic damping characteristics, as should be expected in a linear aeroelastic problem at flow velocities below the flutter speed. On the other hand, the response of the damaged wing exhibits large amplitude, undamped aeroelastic oscillations, typical of limit cycle behavior. Perhaps most important, the oscillatory peak-to-peak amplitudes for the root shear force and bending moment are an order of magnitude larger for the damaged wing as compared to the undamaged wing.

Since for a far field flow velocity 90% of the flutter speed, *i.e.* 110 m/sec, the wing exhibits limit cycle behavior, the next logical step is to evaluate the range of far field flow velocities over which this limit cycle oscillatory behavior occurs. Thus, aeroelastic response to a sharp edged gust was also computed for a flow velocity 85% of the flutter speed, *i.e.* 104 m/sec, and an updraft $W = 8.04\ m/sec$. At this lower flow velocity, the behavior of both undamaged and damaged beams exhibit very similar characteristics. Very slightly higher peak-to-peak vibration amplitude for the root shear force and bending moments are observed, and nearly identical damping levels for both undamaged and damaged beams.

3 Aeroelastic behavior of damaged wing-aileron structures

The focus of the second part of the investigation involves the aeroelastic behavior of wing-aileron systems. As mentioned in the introduction, delaminations induced by foreign object impact, for instance, and the subsequent stiffness reduction, are likely to be particularly significant for control surfaces. Because of the increased importance of three dimensional effects, a more sophisticated aeroelastic model was used for this investigation.

3.1 Aeroelastic Model

To obtain the aeroelastic response of an wing-aileron system, three models were coupled so as to interact at each time step: a structural model, an airloads model, and an inflow model. The state-space inflow model is based on the dynamic inflow theory of Peters [8]. The quality of the inflow model is function of the number of states included in the approximation; 72 inflow states were used in this work.

Another state-space model has been used for predicting the airloads. Details can be found in reference [9]. The model allows for a thin, deformable airfoil performing small arbitrary motions with respect to a reference frame that undergoes arbitrarily large translations and rotations in two dimensions. The airloads are computed at 159 "airstations" along the wing span.

A realistic model of the wing-aileron structure had to be developed. The aileron, modeled with two cubic beam elements, is attached to the wing, modeled with six cubic beam elements, by means of brackets and joints. For smooth operation, the motions of the wing and aileron must be structurally decoupled, *i.e.* the motions of the wing should not induce loads in the aileron structure, yet the lift and drag forces and pitching moment of the aileron must be transfered to the wing. This can be achieved by attaching the aileron to the brackets by means of universal, revolute, prismatic, and spherical joints, as depicted in Fig. 6. The universal and spherical joints at the two ends of the aileron prevent wing angular motions from inducing moments in the aileron. The prismatic joint prevents the occurance of axial forces in the aileron. Finally the revolute joint allows setting the relative rotation of the aileron with respect to the wing. A full validation of this aeroelastic model can be found in [11].

Here again, both undamaged and damaged structures were investigated. It is assumed that the torsional stiffness of the aileron is reduced for the damaged structure. This localized damage is modeled by a nonlinear torsional spring whose properties are depicted in Fig. 2. Such properties would result from the presence of a delamination, for instance. Twisting of the aileron in one direction would induce buckling at the delamination site, resulting in

reduced torsional stiffness, whereas twisting in the other direction would close the delamination, leaving the torsional stiffness unchanged. The reduced torsional stiffness associated with the damage is selected to be half of that of the undamaged aileron. This stiffness reduction appears reasonable in view of the light gage construction of control surfaces.

3.2 Aeroelastic Analysis Results

At first, the flutter behavior of the wing alone is investigated. The physical properties of the wing used in this study are given in Table 2.

To obtain the flutter speed from the numerical simulation, the wing was set at an angle of attack of 0.1 *rad*. Calculations of the response to the sudden onset of lift at time equals to zero were run for various values of the far field flow velocity. At flow velocities below the flutter speed, the wing response is shown to be damped by the aerodynamic forces and eventually settles to a steady-state response. At flow velocities above the flutter speed, the wing response rapidly increases in time and is unstable. By trial and error, the flutter speed can be determined as the air speed for which the wing response seems to be undamped, leading to a periodic response. The flutter speed was found to be about 351 m/sec.

Next, the flutter behavior of the undamaged wing-aileron combination was investigated. The physical properties associated with the aileron are given in Table 3. The wing parameters are the same as in the previous section. At first, the aileron spring stiffness was selected to be very high ($k_\beta = 10^{12}\ Nm/rad$). For this case, the behavior of the wing-aileron structure should be identical to that of the wing alone. Fig. 7 shows the time history of the wing mid-span twist at the flutter speed of 351 m/sec which was found to be identical to that of the wing structure alone. In this figure, the solid line describes the response of the wing, whereas the dashed line gives the corresponding quantity for the aileron.

For values of aileron stiffness above $k_\beta = 10^4\ Nm/rad$ the behaviors of the wing, and wing-aileron models were found to be nearly identical. This was confirmed by the three-degree-of-freedom flutter model applied to the present situation. Fig. 8 shows the predicted non-dimensional flutter speed as a function of non-dimensional aileron frequency $\omega_\beta/\omega_\alpha$ (ω_β

is the aileron deflection frequency,and ω_α is the wing torsional frequency). For large values of the aileron stiffness (that is, large values of ω_β), the flutter speed is nearly independent of the stiffness, whereas below a certain threshold, a very sharp drop in flutter speed occurs when the stiffness decreases. The threshold value is $\omega_\beta/\omega_\alpha \approx 1$, which corresponds to $k_\beta \approx 9 \times 10^3\ Nm/rad$. A simulation was run for $k_\beta = 5 \times 10^3\ Nm/rad$, and the flutter speed was found to be 300 m/sec, confirming the precipitous drop in flutter speed below the threshold stiffness value.

We now turn to the analysis of the flutter behavior of a wing-aileron system damaged by a local delamination. For positive twists, the aileron torsional stiffness is $10^4\ Nm/rad$ but is reduced to $5 \times 10^3\ Nm/rad$ for negative twists, as depicted in Fig. 2 which shows the bi-modular stiffness properties of the damaged aileron for $\sigma = 0.1$ and 0.7. At first, the simulation was run with a sharp stiffness transition, $\sigma = 0.1$.

The first simulation of the damaged wing-aileron system was run at an airspeed $U =$ 360 m/sec. Fig. 9 shows the time history of the wing mid-span twist, as well as the corresponding aileron quantity. Since this airspeed is above the flutter speed for undamaged wing-aileron system, the damaged system is also expected to flutter. This is clearly the case when looking at the time history shown in the figure.

The second simulation of the damaged wing-aileron system was run at an airspeed $U =$ 290 m/sec which is below the flutter speed for the undamaged wing-aileron system. Fig. 10 shows the time history for the wing and aileron mid-span twist. Clearly, the response of the system is stable and damped, although large aileron motions are observed.

The third simulation of the damaged wing-aileron system was run at an airspeed $U =$ 325 m/sec which is below the flutter speed for the undamaged wing-aileron system with $k_\beta = 10^4\ Nm/rad$ but above that for $k_\beta = 5 \times 10^3\ Nm/rad$. At this intermediate airspeed, a limit cycle behavior is observed for the aileron. Figs. 11 and 12 show the time histories for the various quantities in the wing and aileron. The dotted line in the first figure is the total lift per unit span, that is, the sum of the wing and aileron contributions. Although a very slow rise in aileron response is observed, the response does not grow exponentially, as would

be expected if the system were experiencing flutter. Further simulations were conducted at various speeds between 300 and 351 m/sec; and qualitatively similar behavior is observed throughout this airspeed range.

In the above simulation, the parameter σ was kept equal to 0.1, *i.e.* the transition from the low to the high aileron stiffness is rather sharp. Further simulations were run for $\sigma = 0.7$, corresponding to a much smoother transition. The aileron stiffness transitions for these two σ values are shown in Fig. 2. For $\sigma = 0.7$, the airspeed for the onset of limit cycle behavior was found to be about 305 m/sec, as compared with 300 when $\sigma = 0.1$, but qualitatively similar responses were found.

In order to better understand the implications of this limit cycle behavior, bending and twisting moments (at the root for the wing, at the mid-span for the aileron) have been plotted. They are shown in Figs. 13 to 16, for damage characterized by $\sigma = 0.1$. The damaged structure (dashed line) experiences much higher stresses than the undamaged structure (solid line). Thus, the high-frequency limit cycle is likely to produce fatigue problems in the damaged structure much faster than in the undamaged structure. So, even though the flutter speed remains approximately the same for both damaged and undamaged structures, a limit cycle appears at a much lower speed (for the example treated: 300 m/s instead of 351 m/s); and the aircraft flying below the flutter speed with aileron skins delaminated would experience much higher amplitude stress oscillations; up to 10% higher for wing stresses and up to about 50 times larger for aileron stresses. Fatigue life would then seem to be significantly affected.

4 Conclusions

Matrix micro-cracking of composite laminates was found to have a modest effect on the sectional stiffnesses of wings, and on the resulting aeroelastic behavior, though the effect can be very significant on elastic coupling terms. A complicating effect of matrix micro-cracking is that it gives rise to nonlinear material constitutive laws in the presence of nonuniformly

distributed crack densities. In particular, nonlinear, bi-modular sectional stiffness properties are likely to occur in practical situations.

Matrix damage does not seem to have a significant influence on the flutter speed. But for the aeroelastic response to a sharp edged gust, a clear qualitative difference exists between the aeroelastic reponses of the undamaged and damaged wings. The undamaged wing exhibits strong aerodynamic damping characteristics, whereas large amplitude, undamped aeroelastic oscillations, typical of a limit cycle behavior, were observed for the damaged case. At speeds close to, but lower than the flutter speed the peak-to-peak amplitudes for the associated oscillatory root shear force and bending moment are predicted to be as much as an order of magnitude larger for the damaged wing as compared to the undamaged wing. This limit cycle behavior seems to disappear at lower air speeds.

Using a three-dimensional aerodynamic and structural model to simulate wing-aileron flutter when localized delaminations are present, it has been found that the flutter speed of the damaged structure is approximately the same as that of the undamaged structure. But, for a significant range of speed below flutter, high-amplitude oscillations are observed, typical of a limit cycle behavior. These oscillations induce high-amplitude, cyclic stresses in the aileron and at the wing root, that could significantly reduce the fatigue life of the entire structure.

Acknowledgements

The present work was supported by the Air Force Office of Scientific Research under contract #F49620-95-1-0241; Major Brian Sanders was the contract monitor.

References

[1] Ehlers, S.M. and Weisshaar, T.A., "Adaptive Wing Flexural Axis Control." *Proceedings of the Third International Conference on Adaptive Structures*, San Diego, CA, Nov 9-11,

1992, pp 28-40.

[2] Kim T. Atluri S.N., and Loewy R.G., "Modeling of Micro-Crack Damaged Composite Plates Undergoing Nonlinear Bi-Modular Flutter." *AIAA Journal*, To appear.

[3] Laws, N., Dvorak, G.J., and Hejazi, M., "Stiffness Changes in Unidirectional Composites Caused by Crack Sysytems." *Mechanics of Materials*, **2**, 1983, pp 123-137.

[4] Hill, S.C., "A Theory for predicting and Minimizing the Effects of Matrix Degradation on the Thermomechanical Properties of General Laminates." Ph.D. Thesis, Rensselaer Polytechnic Institute, Troy, NY, 1993.

[5] Shyprykevich, P., "Characterization of Graphite/Epoxy Laminates for Aeroelastic Tailoring". *Composite Materials: Testing and Design (Fifth Conference)*, ASTM STP 674, S.W. Tsai, Ed., American Society for Testing and Materials, 1979, pp 40-56.

[6] Giavotto, V., Borri, M., Mantgazza, P., Ghiringhelli, G., Carmaschi, V., Maffioli, G.C., and Mussi, F.,"Anisotropic Beam Theory and Applications", *Computers and Structures*, **16**, 1983, pp 403-413.

[7] Bisplinghoff, R.L., Ashley, H., and Halfman, R.L., "Aeroelasticity", *Addison-Wesley Publishing Comp.*, 1955

[8] Peters, D., and He, C., "Finite State Induced Flow Models, part II: Three-Dimensional Rotor Disk", *J.of A. Vol 32-2*, 1995

[9] Peters, D., and Johnson, M.,"Finite State Airloads for Deformable Airfoils on Fixed and Rotating Wings", *Center for Computational Mechanics of the Washington University*

[10] Bauchau, O.A., and Theron, N.J., "Energy Decaying Scheme for Non-linear Elastic Multi-Body Systems", *Computers and Structures Vol.59 No.2*, 1996

[11] Douxchamps, B., "Nonlinear Aeroelastic Effects in Damaged Composite Aileron-Wing Structures", *Master of Science Thesis*, School of Aerospace Engineering, Georgia Institute of Technology, September 1997

List of Tables

List of Figures

	Torsional	Bending	Coupling
Undamaged Compliance $[m^2/N]$	5.44E-5	3.65E-5	-8.04E-6
Micro-cracked Case 1	37.9%	12.89%	-85.66%
Micro-cracked Case 2	17.14%	6.06%	-38.38%

Table 1: Values of and Per Cent changes in torsional, bending, and coupling compliances for various states.

Wing span $[m]$	2.4
Wing chord $[m]$	0.4
Elastic axis location [%chord]	40
Center of mass location [%chord]	50
Axial stiffness $[N]$	4.35080e+08
Vertical bending stiffness EI $[Nm^2]$	2.32577e+05
Chord-wise bending stiffness $[Nm^2]$	2.98731e+08
Torsional stiffness GJ $[Nm^2]$	2.80514e+04
Sectional mass $[kg/m]$	1.60920e+00
Polar mass moment of inertia I_α $[kg.m^2/m]$	1.19092e-02
Vertical mass moment of inertia $[kg.m^2/m]$	8.60216e-04
Chord-wise mass moment of inertia $[kg.m^2/m]$	1.10490e-02

Table 2: Wing physical properties

Root location on the wing [%span]	33.333
Tip location on the wing [%span]	66.666
Aileron Chord $[m]$	0.1
Hinge location on the chord [%wing chord]	75
Elastic axis location [%aileron chord]	50
Center of mass location [%aileron chord]	50
Axial stiffness $[N]$	4.35080e+08
Vertical bending stiffness EI $[Nm^2]$	2.32577e+05
Chord-wise bending stiffness $[Nm^2]$	2.98731e+08
Torsional stiffness GJ $[Nm^2]$	2.80514e+04
Sectional mass $[kg/m]$	1.60920e-01
Polar mass moment of inertia I_α $[kg.m^2/m]$	1.19092e-02
Vertical mass moment of inertia $[kg.m^2/m]$	8.60216e-04
Chord-wise mass moment of inertia $[kg.m^2/m]$	1.10490e-02

Table 3: Aileron physical properties

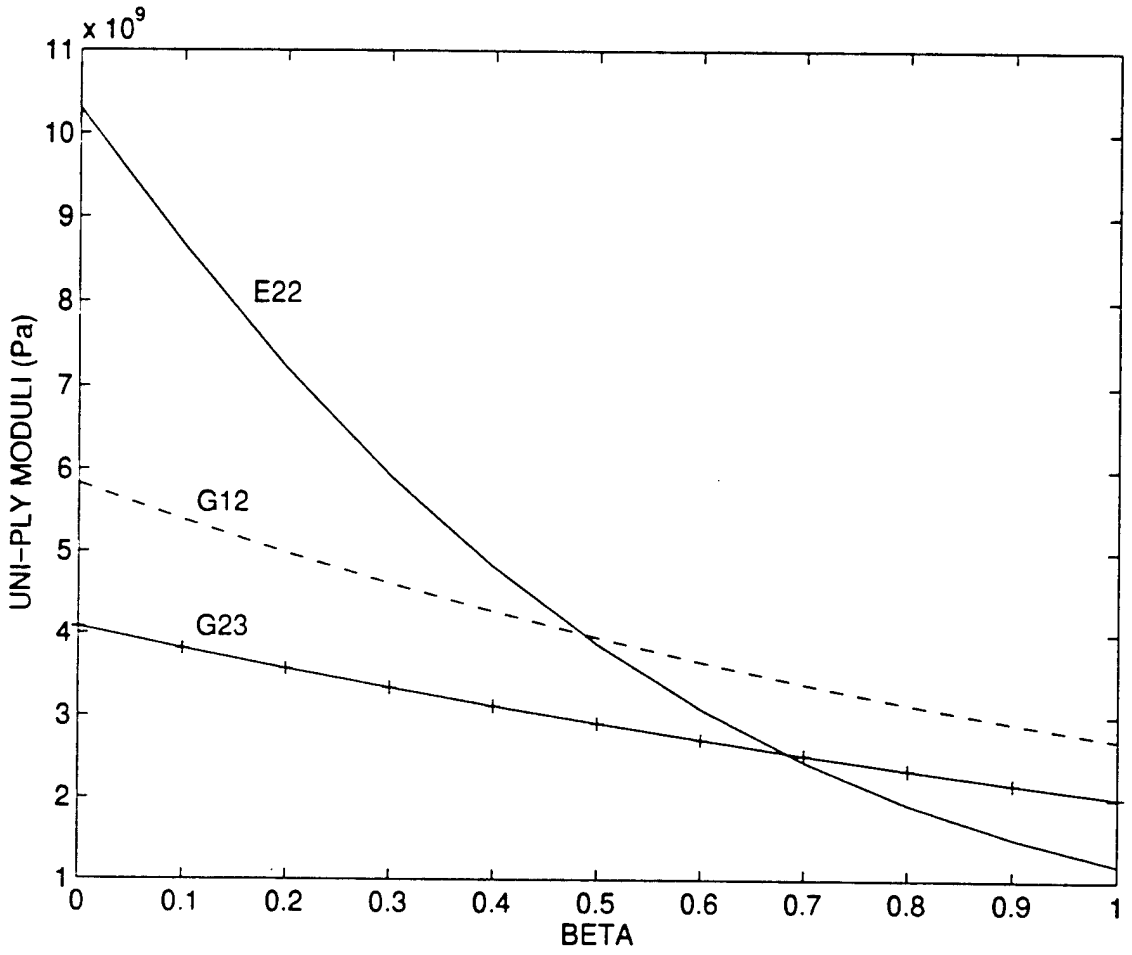

Figure 1: Unidirectional ply stiffness properties as a function of ply crack density.

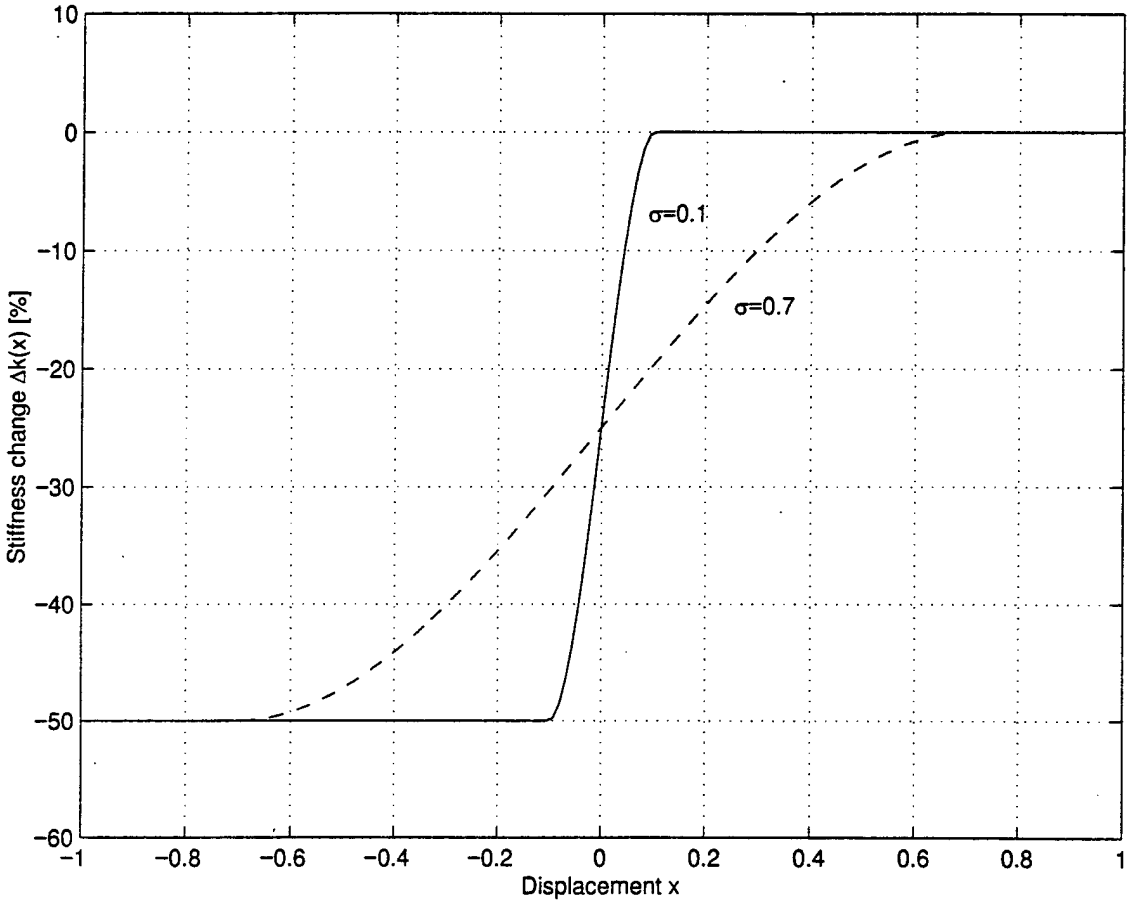

Figure 2: Per Cent changes in stiffness for the damaged and undamaged states

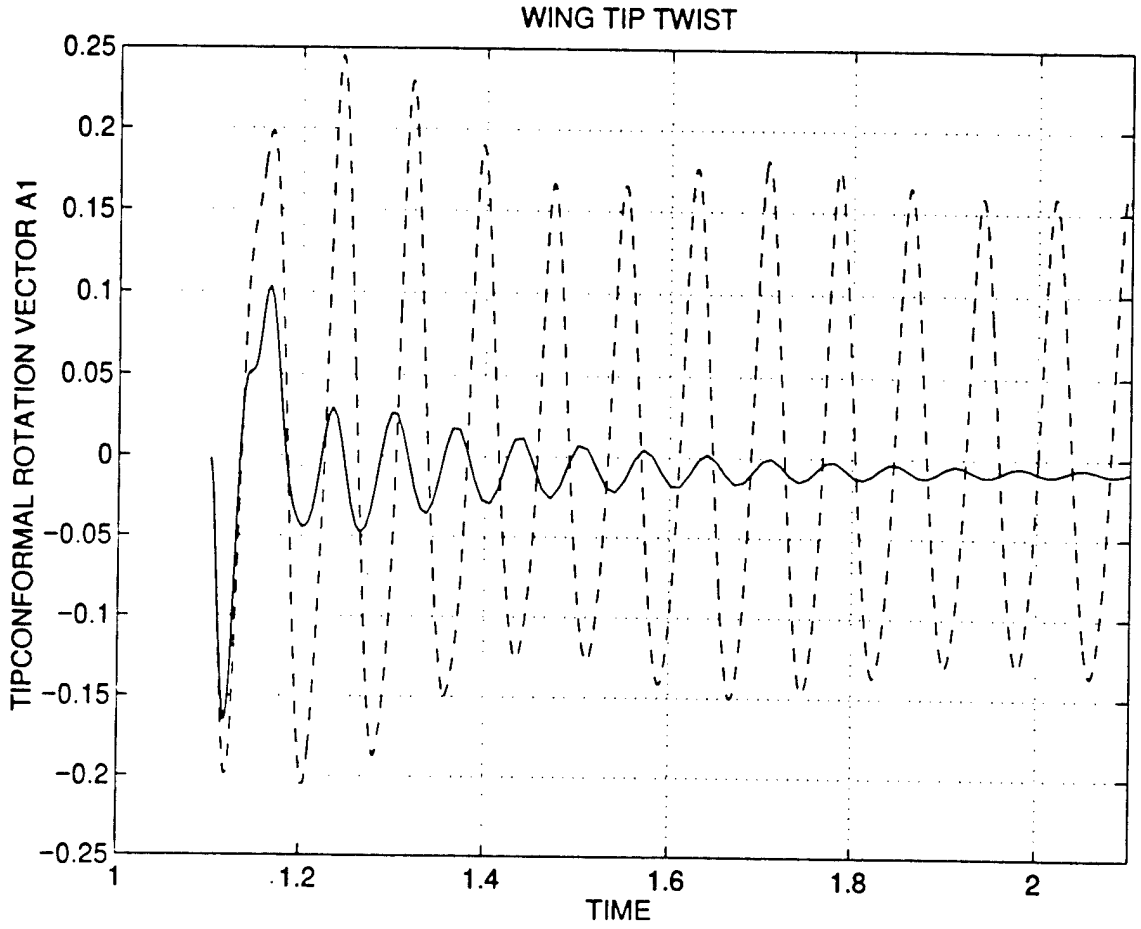

Figure 3: Aeroelastic response to a gust: wing tip rotation (solid line: undamaged wing; dotted line: damaged wing).

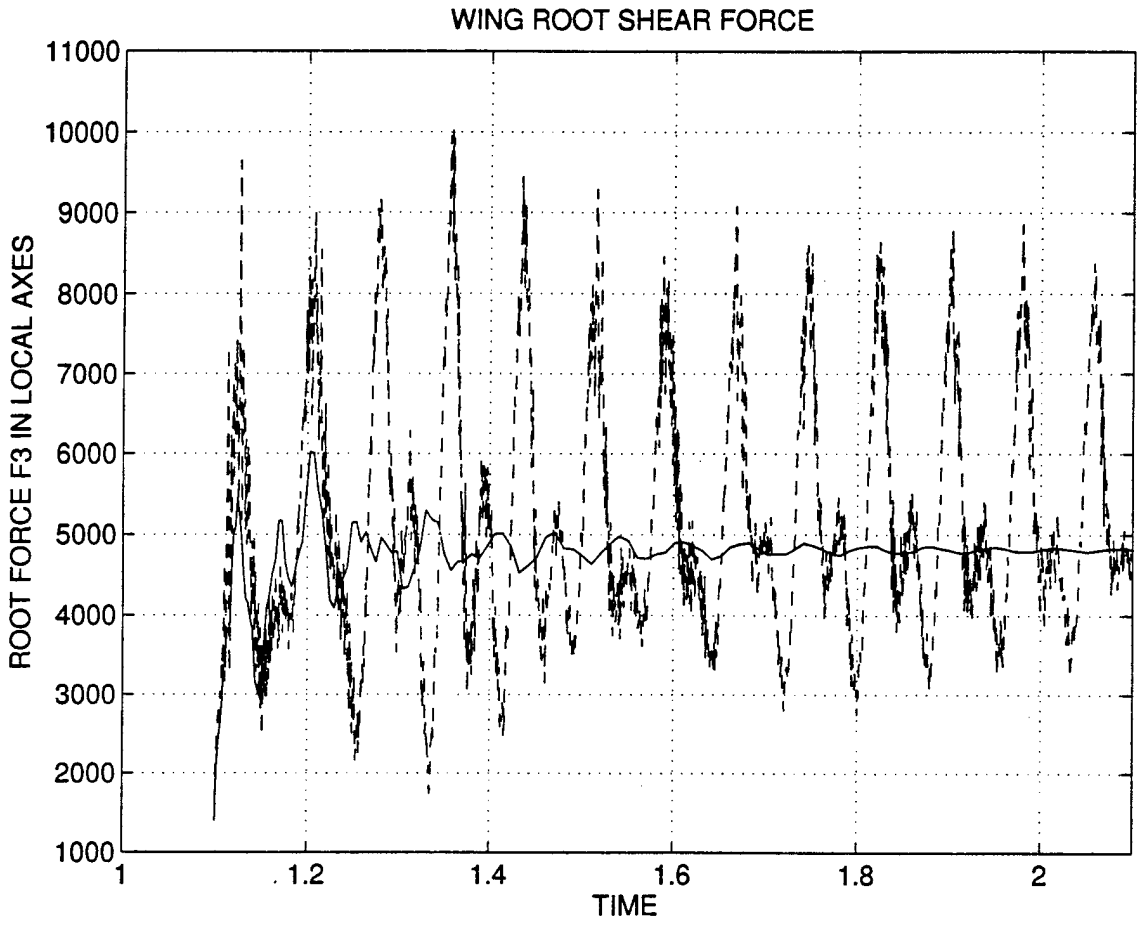

Figure 4: Aeroelastic response to a gust: wing root shear force (solid line: undamaged wing; dotted line: damaged wing).

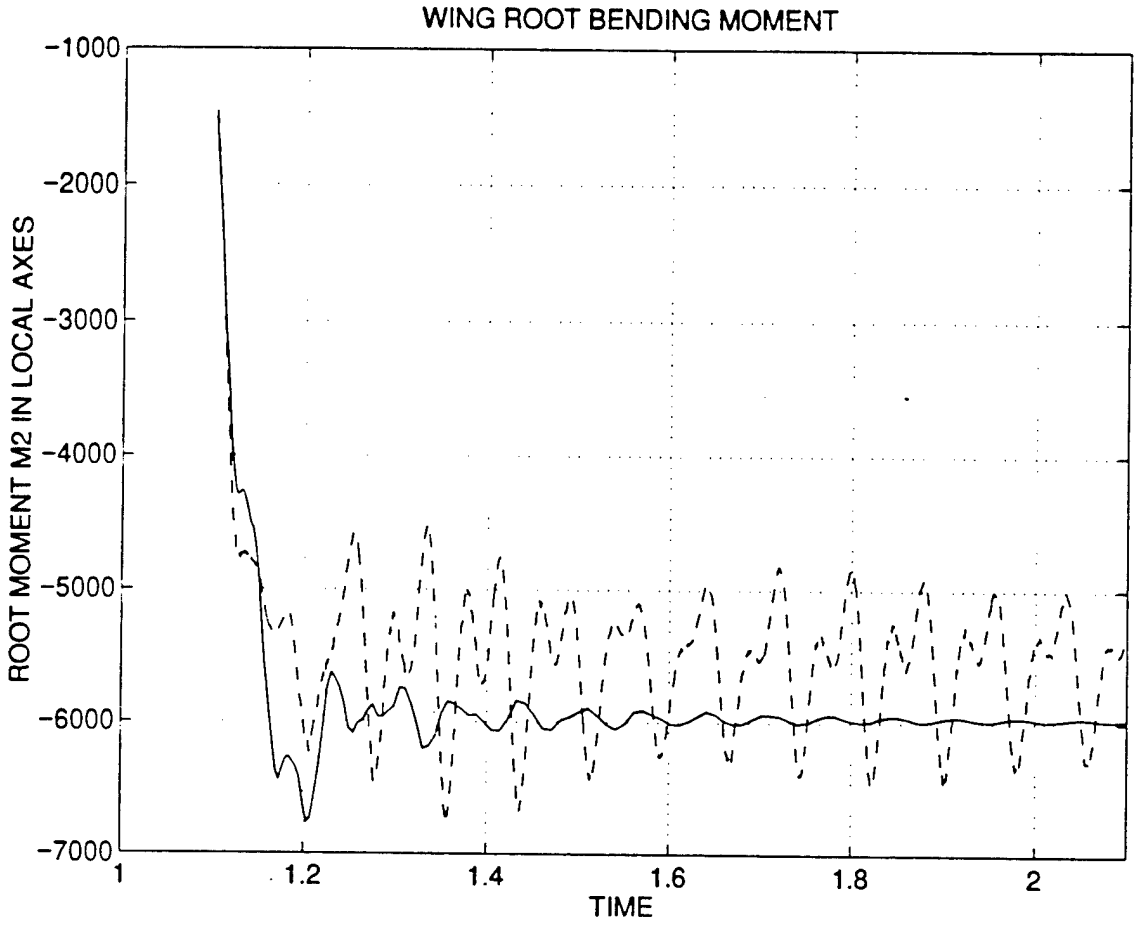

Figure 5: Aeroelastic response to a gust: wing root bending moment (solid line: undamaged wing; dotted line: damaged wing).

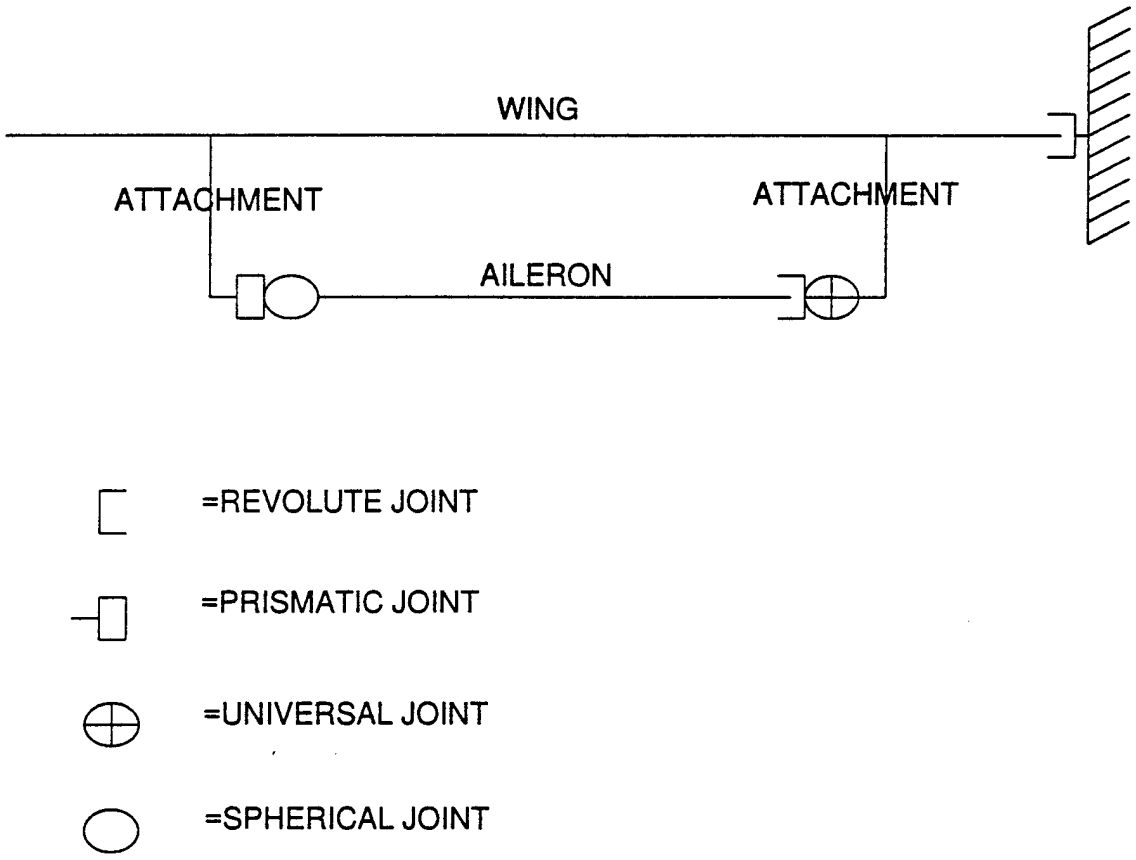

Figure 6: Schematic of the wing-aileron structural model used in the flutter simulations

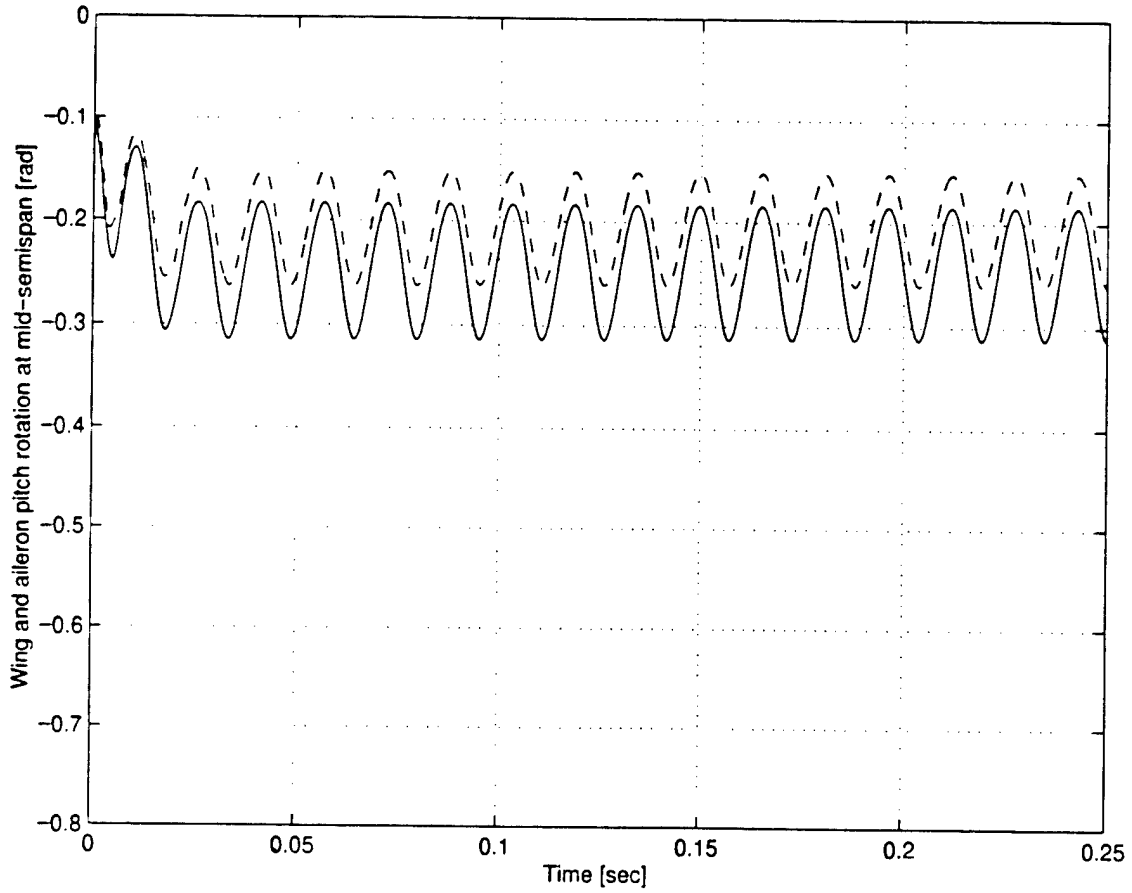

Figure 7: Mid-span pitch rotation time history at flutter speed (351 m/sec) for the wing (solid line) and aileron (dashed line)

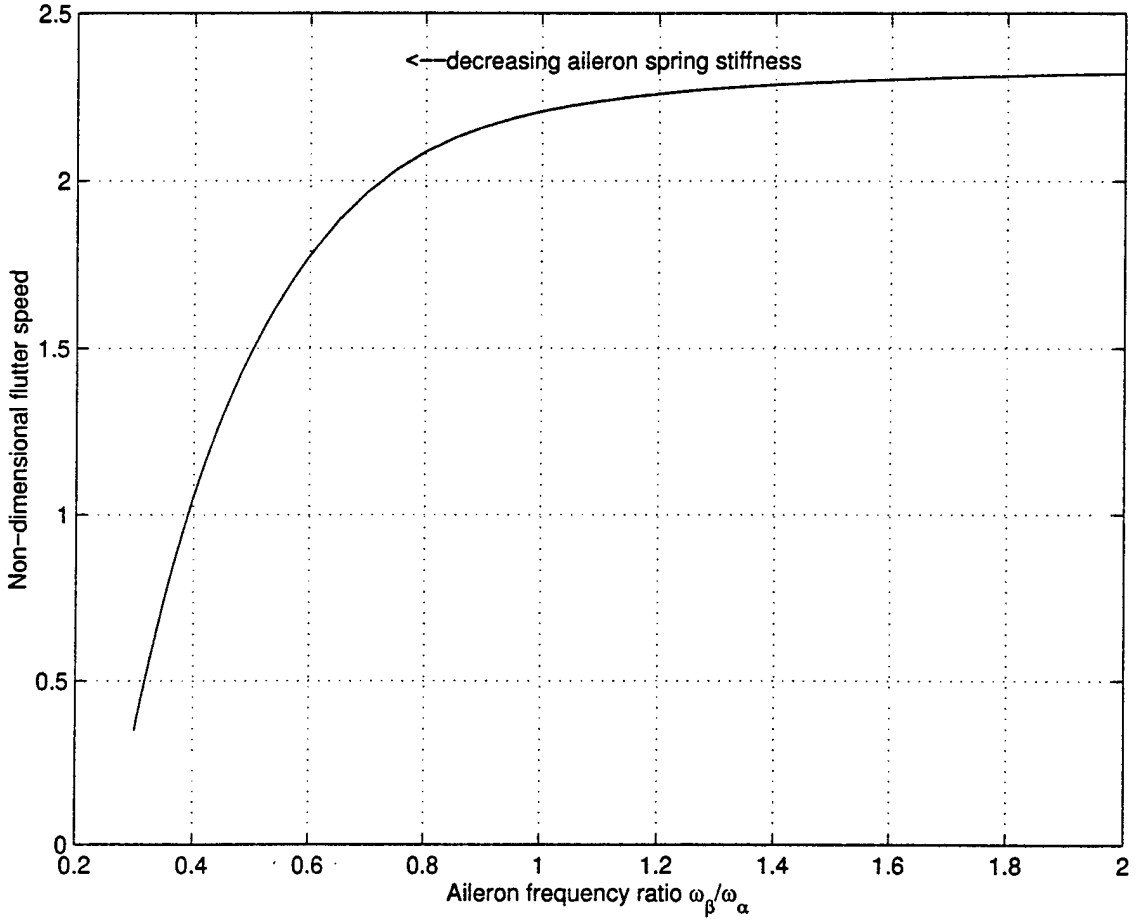

Figure 8: Influence of aileron spring stiffness on the coupled bending-torsion-aileron rotation flutter speed.

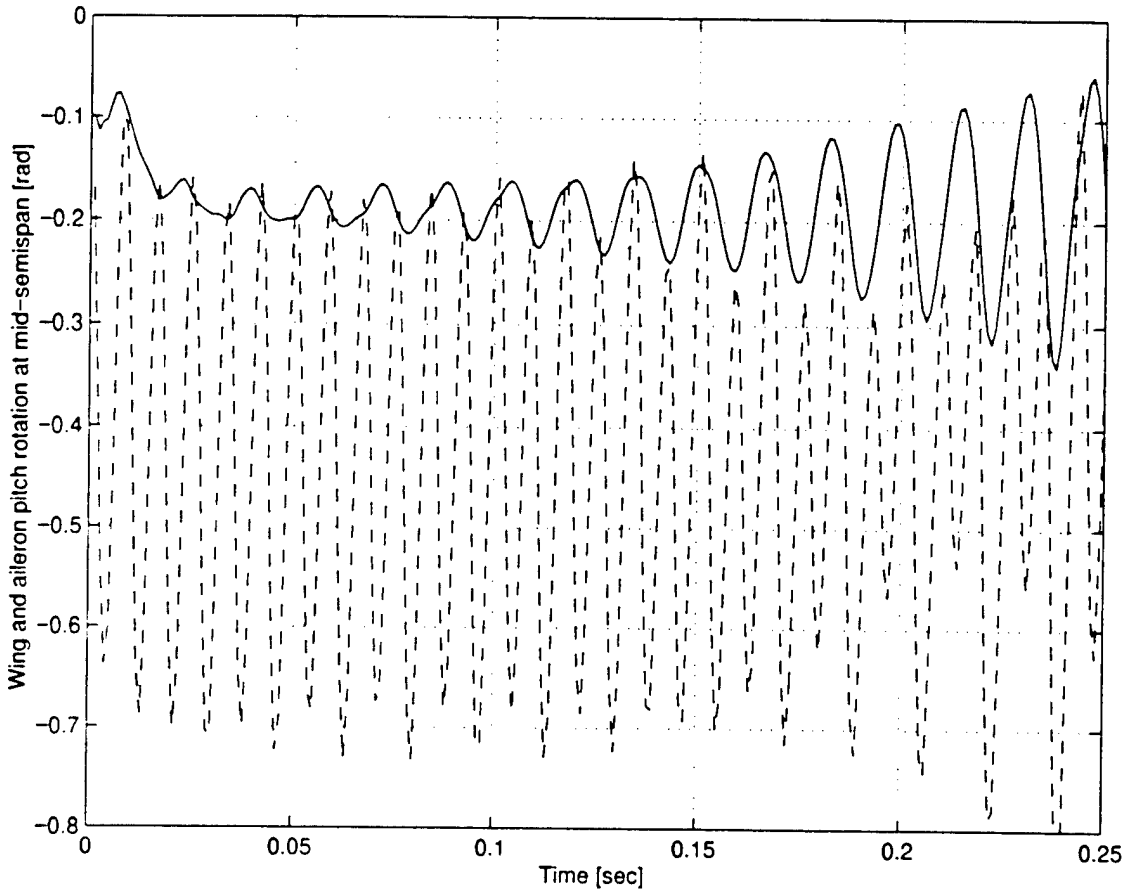

Figure 9: Time history of wing (solid line) and aileron (dashed line) mid-span pitch at $U = 360\ m/sec.$

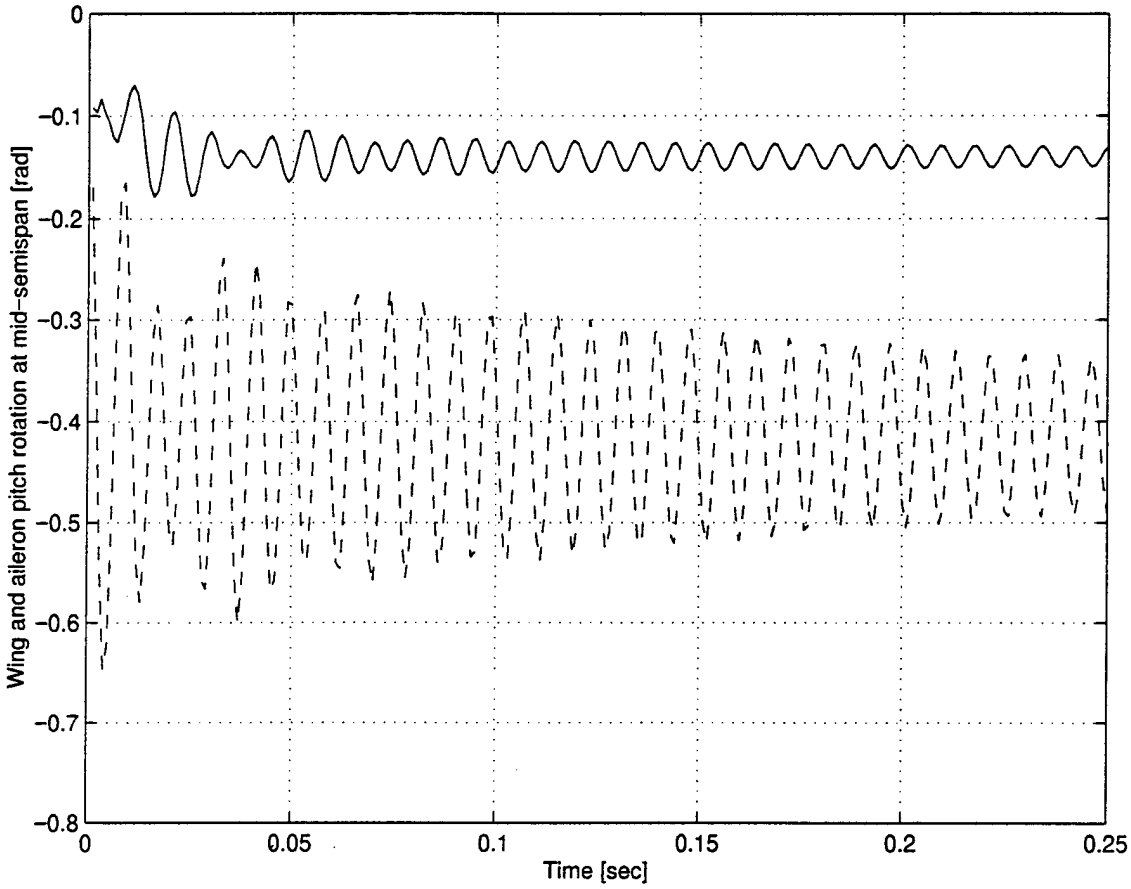

Figure 10: Time history of wing (solid line) and aileron (dashed line) mid-span pitch at $U = 290\ m/sec.$

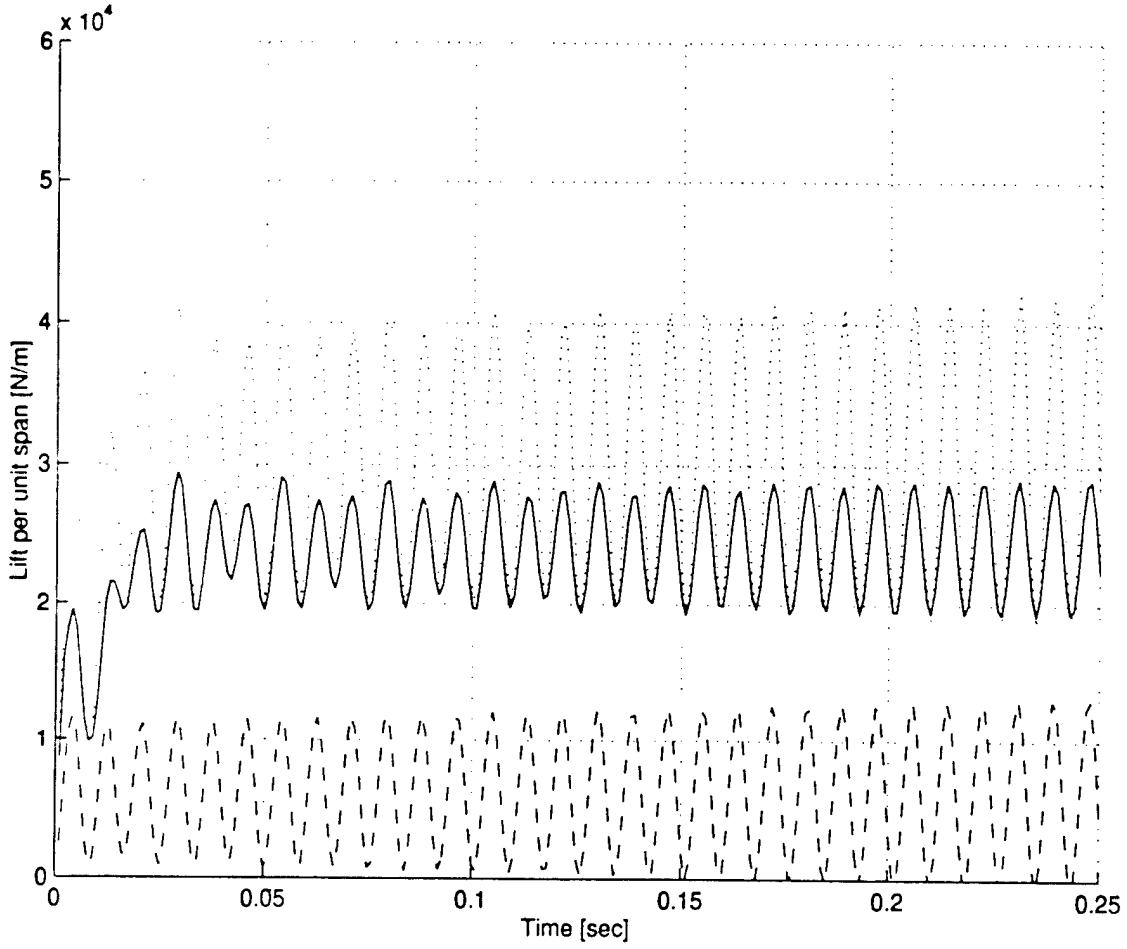

Figure 11: Time history of wing (solid line) and aileron (dashed line) mid-span lift at $U = 325\ m/sec.$

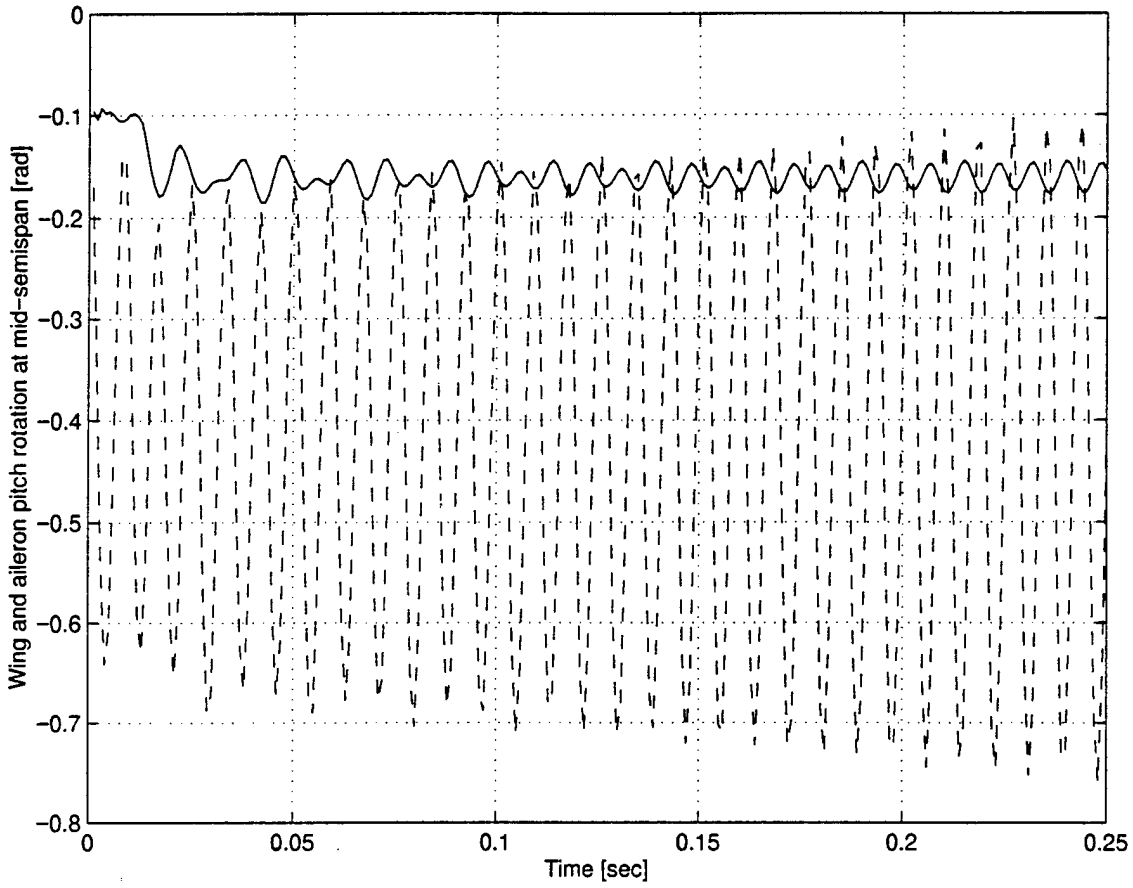

Figure 12: Time history of wing (solid line) and aileron (dashed line) mid-span pitch at $U = 325\ m/sec.$

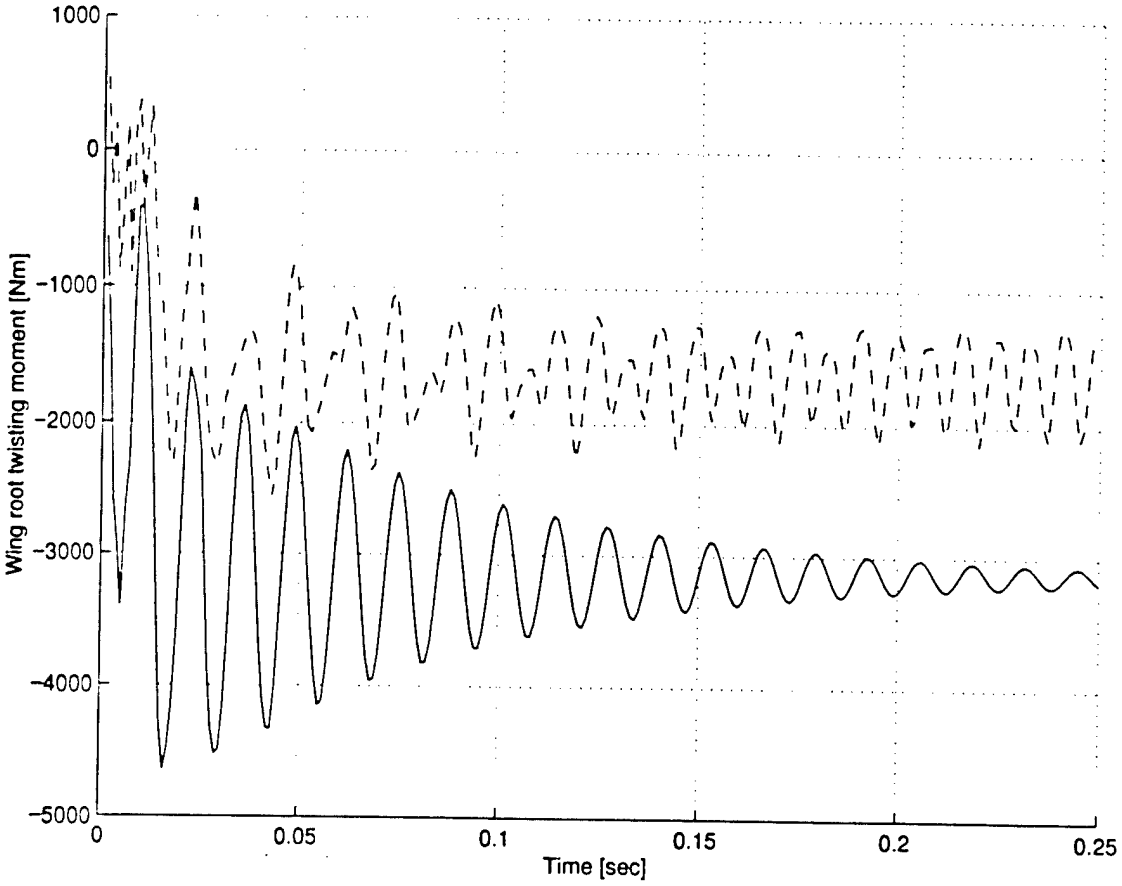

Figure 13: Wing root twisting moment at $U = 325\ m/s$, for the undamaged structure (solid line) and the damaged structure (dashed line)

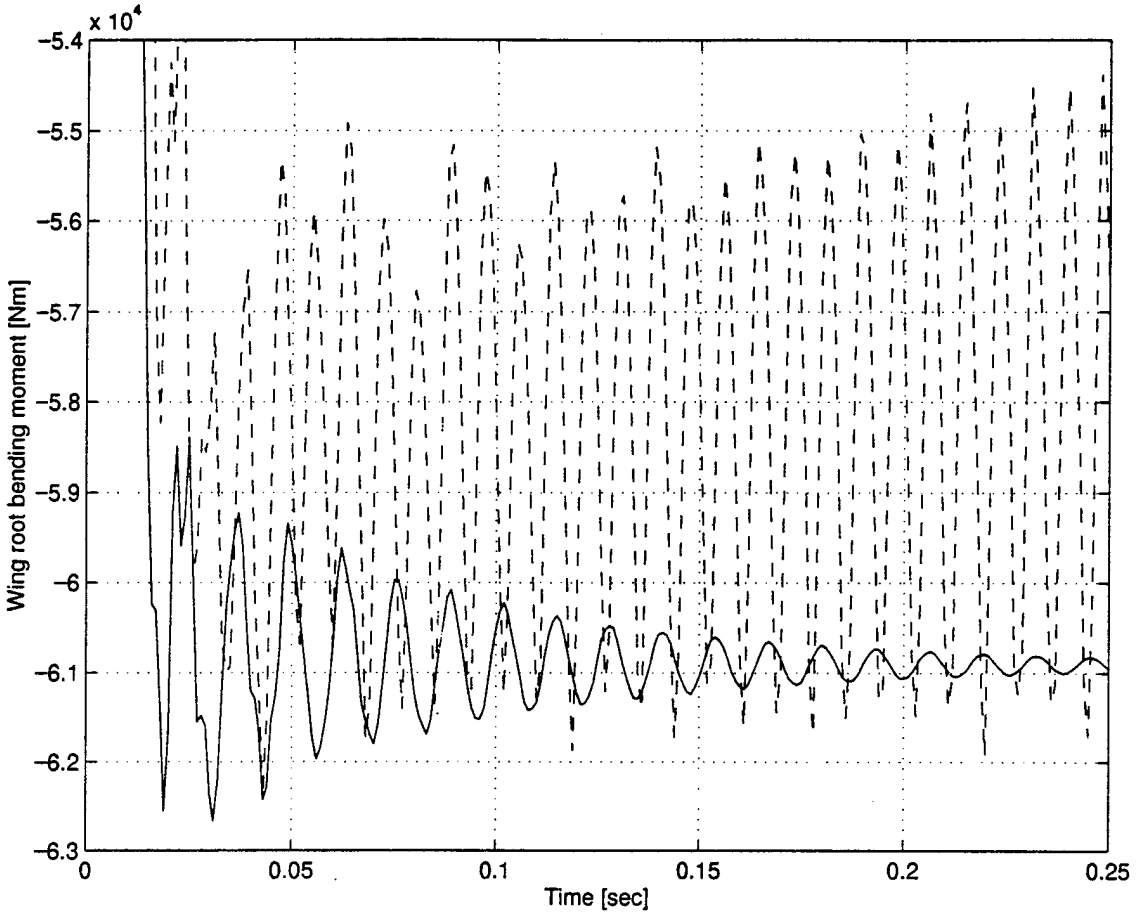

Figure 14: Wing root bending moment at $U = 325\ m/s$, for the undamaged structure (solid line) and the damaged structure (dashed line)

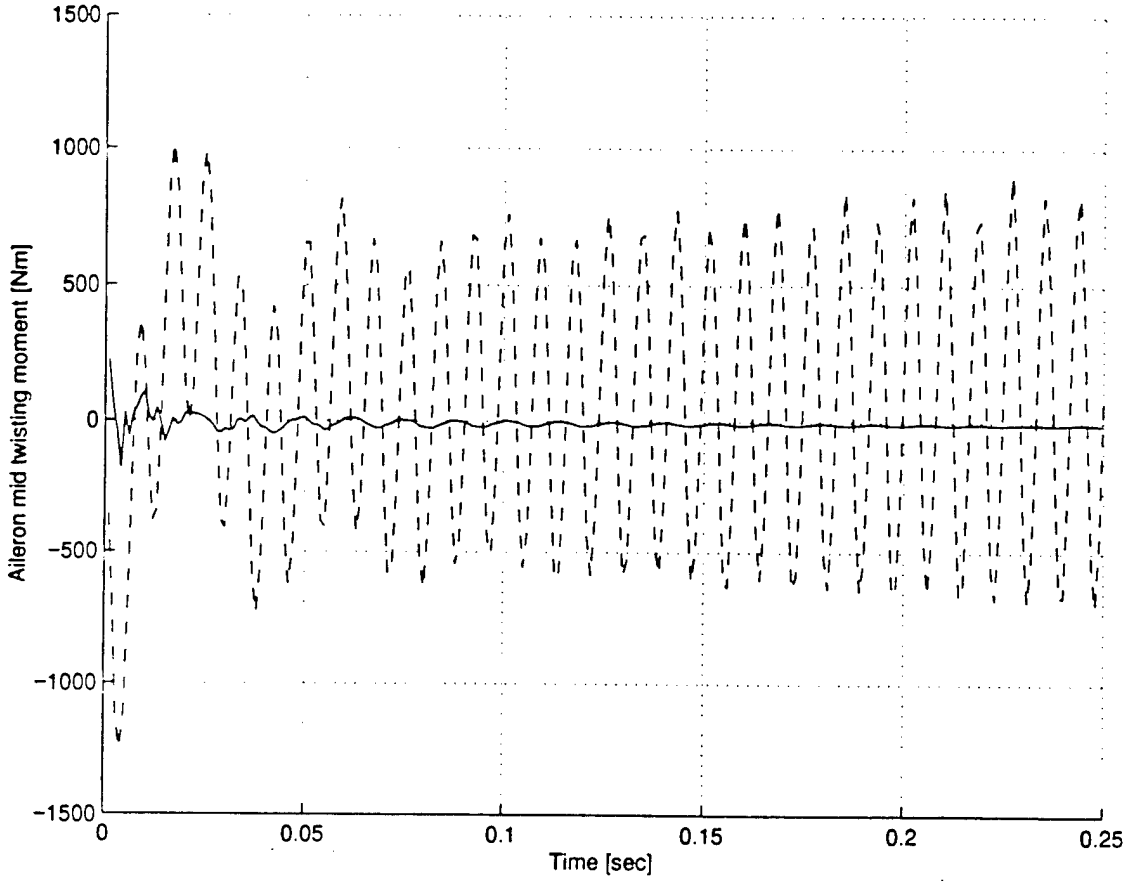

Figure 15: Aileron mid twisting moment at $U = 325\ m/s$, for the undamaged structure (solid line) and the damaged structure (dashed line)

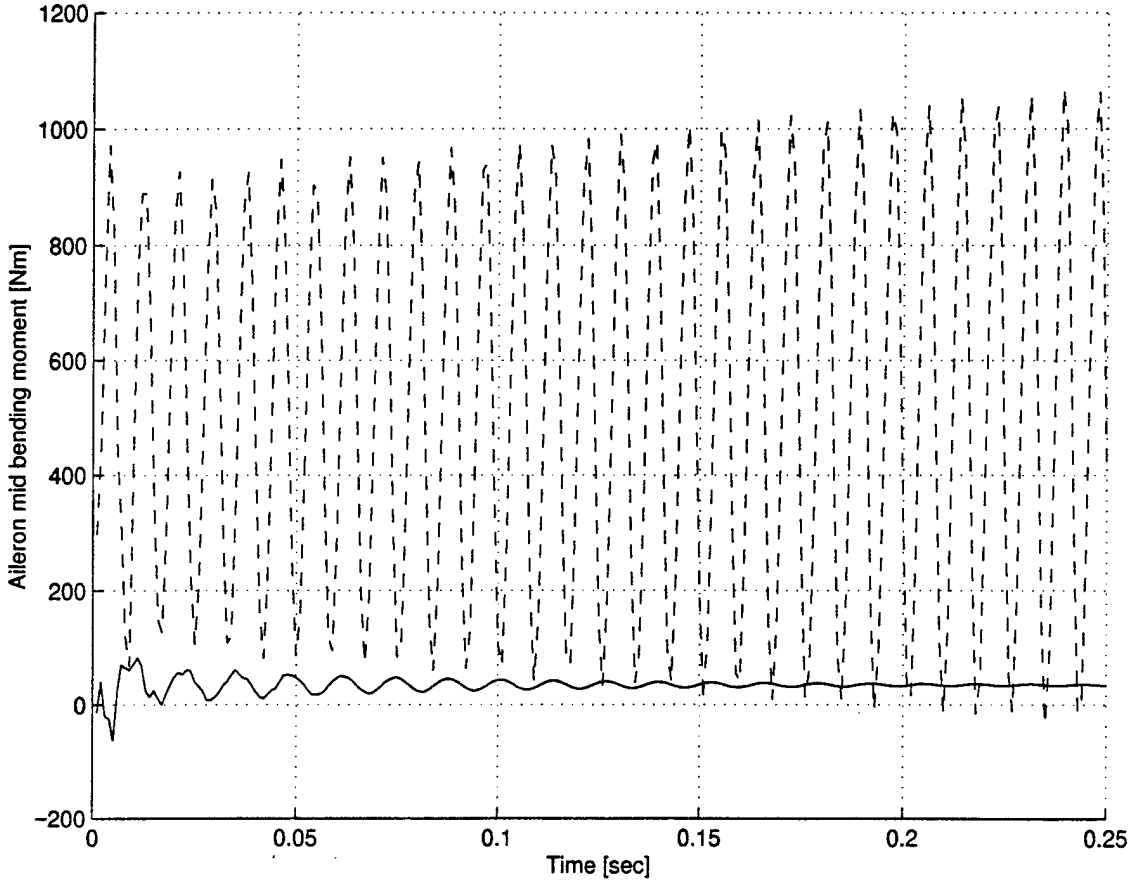

Figure 16: Aileron mid bending moment at $U = 325\ m/s$, for the undamaged structure (solid line) and the damaged structure (dashed line)